PRAMANA
— journal of
physics

Vol. 75, No. 3
September 2010
pp. 471–483

Electron Rydberg wave packets in one-dimensional atoms

SUPRIYA CHATTERJEE, AMITAVA CHOUDHURI, APARNA SAHA and B TALUKDAR*

Department of Physics, Visva-Bharati University, Santiniketan 731 235, India
*Corresponding author. E-mail: binoy123@bsnl.in

MS received 20 September 2009; revised 19 February 2010; accepted 6 April 2010

Abstract. An expression for the transition probability or form factor in one-dimensional Rydberg atom irradiated by short half-cycle pulse was constructed. In applicative contexts, our expression was found to be more useful than the corresponding result given by Landau and Lifshitz. Using the new expression for the form factor, the motion of a localized quantum wave packet was studied with particular emphasis on its revival and super-revival properties. Closed form analytical expressions were derived for expectation values of the position and momentum operators that characterized the widths of the position and momentum distributions. Transient phase-space localization of the wave packet produced by the application of a single impulsive kick was explicitly demonstrated. The undulation of the uncertainty product as a function of time was studied in order to visualize how the motion of the wave packet in its classical trajectory spreads throughout the orbit and the system becomes nonclassical. The process, however, repeats itself such that the atom undergoes a free evolution from a classical, to a nonclassical, and back to a classical state.

Keywords. One-dimensional Rydberg atom; half-cycle pulse; wave-packet dynamics.

PACS Nos 32.80.Rm; 31.15.Gy; 03.65.Ge

1. Introduction

When atoms are placed in an intense electric field, the orbital electrons usually occupy states of large principal quantum numbers often called the high Rydberg states. These states, by interaction with half-cycle pulses, can produce wave packets of the desired form [1]. The Rydberg wave packets thus formed, on the one hand, have a number of applicative relevance [2] and, on the other hand, tend to throw new light on the correspondence between classical and quantum mechanics [3]. Thus engineering Rydberg states by half-cycle pulses has been a subject of extensive theoretical investigation [4].

The half-cycle pulse (HCP) comprises a strong unidirectional electric field, the duration t_p of which is much shorter than the classical orbital period t_n of the initial Rydberg state $|n\rangle$ that interacts with the HCP to produce the wave packet. Once a

Rydberg wave packet is formed by interaction with the HCP, its motion is periodic with the same classical period $t_{\rm n}$ or $t_{\rm cl}$ as that of a charged particle in the Coulomb field. This motion, however, lasts for only a few cycles, whereupon quantum interference effects cause the wave packet to first collapse and then to undergo a sequence of revivals presumably because the atomic eigenspectra are not equispaced. The collapse and revival phenomena leave their signature on the widths of the position and momentum distributions of the wave packet. In particular, they become oscillatory functions of time so as to produce a time-dependent uncertainty product. The object of the present work is to investigate these points in some detail for the interaction of HCP with the Rydberg electrons of a one-dimensional (1D) atom. The classical phase-space structure of this simplified atomic model has been found to closely mimic the three-dimensional systems for initial conditions representing elongated Stark orbits [5]. In view of this, analytical treatment for studying the properties of 1D Rydberg atoms interacting with HCP is yet an interesting curiosity [4].

For half-cycle pulses $t_{\rm p} \ll t_{\rm cl}$, and so each pulse essentially delivers an impulsive momentum q to the electron in the Rydberg state $|n\rangle$. Consequently, we can use the form factors [6]

$$T_{n'n}(q) = \langle n'|{\rm e}^{iqx}|n\rangle \tag{1}$$

for the weight factors in superposing energy eigenstates to construct the wave packet for a 1D atom. In terms of these transition amplitudes the Rydberg wave packet $\psi(x,t)$ can be written as

$$\psi(x,t) = \sum_{n'} {\rm e}^{-iE_{n'}t}|n'(x)\rangle T_{n'n}, \quad |n'(x)\rangle = \langle x|n'\rangle. \tag{2}$$

Because the 1D atoms are formed by the photoexcitation of the extreme Stark states of high-n manifold in the presence of a weak DC electric field [7], the corresponding classical trajectory lies on a line at one side of the atomic core. In other words, the atomic potential provides an infinite barrier at $x = 0$ such that the motion is confined to the $x > 0$ region of the phase space. The eigenvalues of the 1D Hamiltonian are $E_n = -1/2n^2$ with the corresponding eigenfunctions given by

$$|n(x)\rangle = \frac{2x}{\sqrt{n^3}}{\rm e}^{-x/n}{}_1F_1\left(-n+1, 2; \frac{2x}{n}\right). \tag{3}$$

Here ${}_1F_1(\cdot)$ stands for the confluent hypergeometric function. In writing the expressions for E_n and $|n(x)\rangle$ we have chosen to work with atomic units. Using (3), the matrix element in (1) can be evaluated analytically and has been given in the classic text on quantum mechanics by Landau and Lifshitz [8]. The expression given in ref. [8] can, in principle, be used to find expectation values of position and momentum operators like $\langle x\rangle$, $\langle x^2\rangle$, $\langle p\rangle$ and $\langle p^2\rangle$. For the position operator the mean value is given by

$$\langle x\rangle = \sum_{jj'} T^*_{j'i}T_{ji}x_{j'j}{\rm e}^{iwt}, \quad w = E_{j'} - E_j, \tag{4}$$

where the expectation value has been taken between two Rydberg wavepackets labelled by (j, i) and (j', i). The matrix element $x_{fi} = \langle f|x|i\rangle$ can, formally, be evaluated from

$$x_{fi} = i \lim_{q\to 0} \frac{\partial T_{fi}}{\partial q}. \tag{5}$$

It is easy to see that if one tries to obtain x_{fi} using the transition matrix elements of Landau and Lifshitz [8], the calculation of diagonal and off-diagonal terms requires separate considerations. In particular, x_{ii} calculated using (5) exhibits an awkward singularity although $\langle i|x|i\rangle$ represents a well-defined function. We note that the expression for $T_{n'n}$ evaluated in the semiclassical approximation by the method of stationary phase is free from this problem and has been used by Bersons and Veilande [6] to reproduce experimental results of Wetzels *et al* [9] on the interaction of Rydberg atoms with half-cycle pulses. It is quite straightforward however to derive an exact expression for the transition matrix element that can be used to evaluate the limit in (5) unambiguously for both $f = i$ and $f \neq i$. In §2 we present such an exact analytical result for $T_{nn'}$. As a useful application of this matrix element we then construct closed form expressions for the expectation values of x, x^2, p and p^2 that characterize the widths $\sigma_x = \Delta x = \sqrt{\langle x^2\rangle - \langle x\rangle^2}$ and $\sigma_p = \Delta p = \sqrt{\langle p^2\rangle - \langle p\rangle^2}$ of the position and momentum distributions. In §3 we study the evolution and revival structure of the localized quantum wave packet following the application of a kick. To provide an insight into the transient phase-space localization [10] of the wave packet, we also study the time development of the widths of the position and momentum distributions. Our results for the uncertainty product as a function of time exhibit a cyclic evolution. The localized quantum wave packet initially follows the corresponding classical motion. As time increases the uncertainty product first increases such that the packet becomes purely quantum mechanical and then decreases; the motion becomes classical again. Finally, in §4 we summarize our outlook on the present work and make some concluding remarks.

2. Transition matrix elements and expectation values of position and momentum operators

The expression for the transition matrix element in (1) as given in Landau and Lifshitz [8] is calculated first by transforming the integrand by the recurrence relation [11]

$$z\,{}_1F_1(a, b+1, z) = b\,{}_1F_1(a, b, z) - b\,{}_1F_1(a-1, b, z) \tag{6}$$

for the confluent hypergeometric function and then making use of the integral [12]

$$\begin{aligned}
&\int_0^\infty \mathrm{e}^{-\lambda z} z^{\gamma-1}\,{}_1F_1(\alpha, \gamma, kz)\,{}_1F_1(\alpha', \gamma, k'z)\,\mathrm{d}z \\
&\quad = \Gamma(\gamma)\lambda^{\alpha+\alpha'-\gamma}(\lambda-k)^{-\alpha}(\lambda-k')^{-\alpha'} \times\ {}_2F_1(\alpha, \alpha', \gamma, y), \\
&y = \frac{kk'}{(\lambda-k)(\lambda-k')}, \quad \lambda > 0.
\end{aligned} \tag{7}$$

The argument of the Gaussian hypergeometric functions ${}_2F_1(\cdot)$ which occur in the result for $T_{n'n}$ in ref. [8] is given by

$$y = -\frac{4nn'}{(n-n')^2 + q^2n^2n'^2}. \tag{8}$$

Clearly, $\lim_{q\to 0} y$ becomes infinity for $n' = n$. It may appear that a linear transformation like

$${}_2F_1(a,b;c;y) = (1-y)^{-a}\,{}_2F_1\left(a, c-b; c; \frac{y}{y-1}\right)$$

or

$${}_2F_1(a,b;c;y) = (1-y)^{-b}\,{}_2F_1\left(c-a, b; c; \frac{y}{y-1}\right)$$

will remove the singularity in $T_{n'n}$ that arises through the hypergeometric function. But we note that in this case the singularity is transferred from ${}_2F_1(a, c-b; c; \frac{y}{y-1})$ or ${}_2F_1(c-a, b; c; \frac{y}{y-1})$ to the factors $(1-y)^{-a}$ or $(1-y)^{-b}$ where a and b are negative integers [8]. As a result we need separate considerations to evaluate the diagonal and off-diagonal matrix elements of x_{fi} in (5). However, it is rather straightforward to get rid of this problem.

The confluent hypergeometric function in (3) is a polynomial and can, therefore, be written as

$${}_1F_1(-p,c,z) = \Gamma(c)\sum_{r=0}^{p}(-1)^r \begin{pmatrix} p \\ r \end{pmatrix} \frac{z^r}{\Gamma(c+r)}, \quad \begin{pmatrix} p \\ r \end{pmatrix} = {}^pC_r. \tag{9}$$

Expanding one of the ${}_1F_1(\cdot)$ functions according to (9), the integral in (1) can be evaluated in terms of

$$\int_0^\infty x^{\sigma-1}\mathrm{e}^{-\mu x}\,{}_1F_1(a,c,\lambda x)\mathrm{d}x = \frac{\Gamma(\sigma)}{\mu^\sigma}\,{}_2F_1\left(a,\sigma,c,\frac{\lambda}{\mu}\right), \quad \sigma \geq 1, \quad \mu > 0 \tag{10}$$

to write

$$T_{n'n} = \alpha_{n'n}\sum_{r'=0}^{n'-1}\beta_{r'n'}f_{m'n'n}(q), \quad \alpha_{n'n} = \frac{4}{\sqrt{n^3n'^3}}, \quad m' = r'+3. \tag{11}$$

Here

$$\beta_{r'n'} = \left(-\frac{2}{n'}\right)^{r'}\frac{1}{\Gamma(r'+2)}\begin{pmatrix} n'-1 \\ r' \end{pmatrix} \tag{12a}$$

and

$$f_{m'n'n}(q) = \frac{\Gamma(m')}{y(q)^{m'}}\,{}_2F_1\left(-n+1, 3+r', 2, \frac{2}{n}y(q)^{-1}\right) \tag{12b}$$

with

$$y(q) = \left(\frac{1}{n} + \frac{1}{n'} - iq\right). \tag{13}$$

Clearly, at $q = 0$, $T_{n'n}$ are well-defined functions for both $n' = n$ and $n' \neq n$ such that the expression in (11) provides an uncomplicated basis to compute x_{fi} by using (5). In close analogy with the expression for $\langle x\rangle$ in (4), the expressions for $\langle x^2\rangle$, $\langle p\rangle$ and $\langle p^2\rangle$ will require the knowledge of $x^2_{fi} = \langle f|x^2|i\rangle$, $p_{fi} = -i\langle f|\frac{\mathrm{d}}{\mathrm{d}x}|i\rangle$ and $(p^2)_{fi} = -\langle f|\frac{\mathrm{d}^2}{\mathrm{d}x^2}|i\rangle$ respectively. We have obtained the results for x_{fi} and $(x^2)_{fi}$ in the form

$$(x^s)_{n'n} = \alpha_{n'n} \sum_{r'=0}^{n'-1} \beta_{r'n'} f_{m'+sn'n}(0), \quad s = 1, 2. \tag{14}$$

Similar expressions for p_{fi} and $(p^2)_{fi}$ are somewhat lengthy and are given in Appendix A.

3. Evolution of wave packets and related observables

From eqs (2), (4), (5), (14), (A1) and (A2) it is evident that evolution properties of the wave packet and $\langle x^n\rangle$, $\langle p^n\rangle$ etc. depend sensitively on the values of the transition matrix elements $T_{n'n}$ for which we presented an expression alternative to that given in Landau and Lifshitz [8]. Thus, it is important to compare the numerical results of $T_{n'n}$ as computed from these two separate expressions. Because of this, we plot in figure 1 the values of $|T_{n'n}|$ obtained from (11) as a function of n' for $n = 25$. We have chosen to work with three different values of q, 0.0010, 0.0016 and 0.0020 a.u., and used dotted, solid and dashed lines to represent the corresponding curves for $|T_{n'n}|$. Note that $q = 0.0016$ a.u., corresponds to $qn^2 = 1$, a relation often used in the weak electric field limit [6] when only a few neighbouring states are populated. From this figure we see that the curves for $|T_{n'n}|$ becomes more and more peaked at the centre ($n = 25$) and flat on the wings as the value of q decreases. We have verified this behaviour of the transition matrix elements by using the expression in ref. [8] and, more significantly found that the two sets of numbers for $T_{n'n}$ as computed from the alternative expressions for the matrix elements agree to within eight places of decimal. We can, therefore, safely use (11) to study the time evolution of wave packets according to (2).

As figure 1 shows that the transition probabilities or form factors are strongly centred around the kicked state n, only those states with energies $E_{n'}$ near E_n enter appreciably into the sum in (2). A Taylor series expansion of $E_{n'}$ about E_n introduces distinct time scales that depend on n and we have [13]

$$t_{\mathrm{cl}} = \frac{2\pi}{|E'_n|}, \quad t_{\mathrm{rev}} = \frac{2\pi}{\frac{1}{2}|E''_n|} \quad \text{and} \quad t_{\mathrm{sr}} = \frac{2\pi}{\frac{1}{6}|E'''_n|}, \tag{15}$$

where the primes on E_n denote differentiation with respect to n. The first time scale t_{cl} stands for the classical period while t_{rev} and t_{sr} refer to revival and super-revival times of the wave packet. The time scales in (15) in conjunction with the Taylor expansion of $E_{n'}$ can be used to rewrite (2) in the form

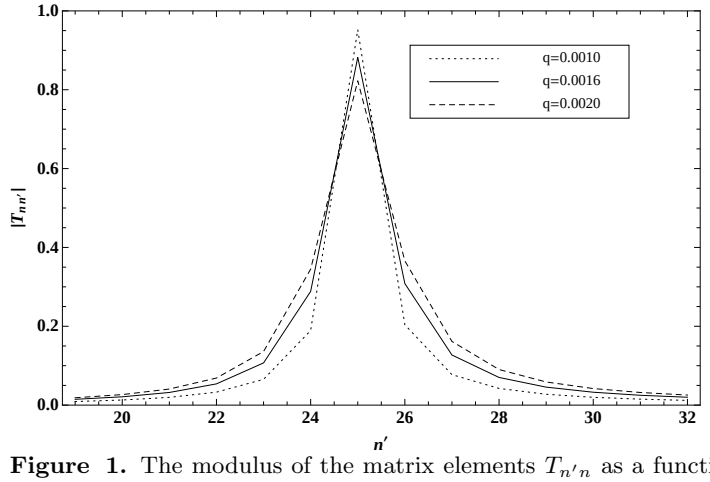

Figure 1. The modulus of the matrix elements $T_{n'n}$ as a function of n' for $n = 25$ and three different values of q, 0.0010, 0.0016 and 0.0020 a.u.

$$\psi(x,\,\tau) = \sum_{n'} T_{n'n}|n'(x)\rangle \mathrm{e}^{[-2\pi i\{(n'-n)\tau + \frac{3}{2n}(n'-n)^2\tau + \frac{2}{n^2}(n'-n)^3\tau\}]} \qquad (16)$$

with the scaled time $\tau = t/t_{\mathrm{cl}}$.

There are three terms inside the curly brackets in the phase of $\psi(x,\,\tau)$ associated with the time scales t_{cl}, t_{rev} and t_{sr} respectively. In this context, let us divide the wave packet into three different categories designated by $\psi_i(x,\tau)$, $i = 1, 2$ and 3. The index i denotes the number of terms added in order in the phase of $\psi(x,\tau)$. Figure 2 shows the evolution of a wave packet created by the HCP delivering momentum $q = 0.0016$ a.u. to a Rydberg electron at the excited state $n = 25$. The wave packet involves a manifold of seven Stark states with $22 \leq n' \leq 28$. We have, in this figure, plotted $|\psi_i(x,\,\tau)|^2$, $i = 1, 2$ and 3 as a function x/n^2 for scaled times $\tau = 0$, 10, 16.3, 100 and 300 by using solid, dotted and dashed lines for $|\psi_1(x,\,\tau)|^2$, $|\psi_2(x,\tau)|^2$ and $|\psi_3(x,\,\tau)|^2$. Figure 2a gives the evolution at $\tau = 0$. As expected, the curves for $\psi_1(x,\,\tau)$, $\psi_2(x,\,\tau)$ and $\psi_3(x,\,\tau)$ coalesce for $\tau = 0$ and give rise to a single solid curve representing evolution of the initial wave packet. With the advent of time $|\psi_i|^2$'s split off. This is apparent for the curves in figure 2b for $\tau = 10$. At $\tau = 16.3$ the curves for $|\psi_i|^2$'s again coalesce (figure 2c) showing revival of the initial wave packet. After $\tau = 16.3$ we again have different spatial evolution of the three components (figure 2d, $\tau = 100$). But interestingly, the curves for $|\psi_i|^2$'s again tend to coalesce at $\tau = 300$ (figure 2e) so as to leave a signature for super-revival. Our results of τ for revival and super-revival are in close agreement with those obtained from (15) which gives $\tau = 16.67$ and 312.5.

Following the line of numerical calculation of Wetzels *et al* [9] we used our expression for T_{fi} to determine the expectation values of x and x^2 by wave packets freely evolving in time. As in figure 2 we assume that the wave packet was created from the Stark states $n = 25$ by an HCP with $q = 0.0016$ a.u. Further, the initial population was assumed to be redistributed to the manifold of seven Stark states ($22 \leq n \leq 28$). We shall use these data in all subsequent discussions. Figures 3a and 3b show the plot of $\langle x\rangle$ and $\langle x^2\rangle$ as calculated from (14) as a function of scaled

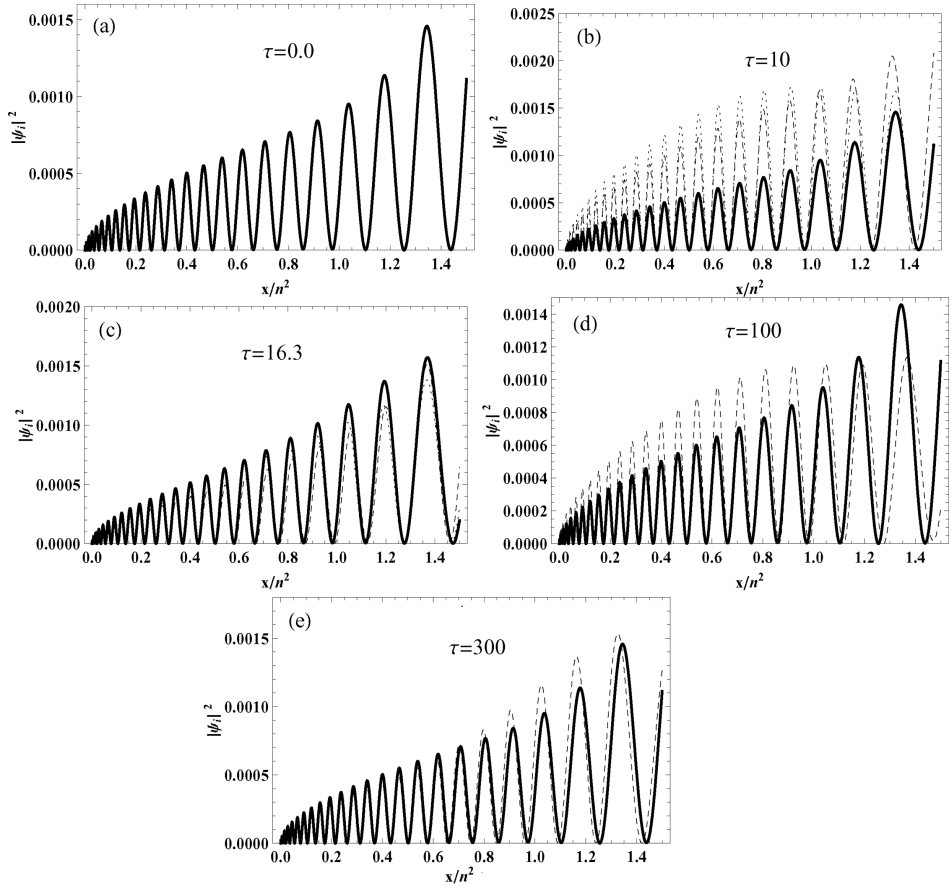

Figure 2. Wave packet produced from the kicked Rydberg state $n = 25$ calculated by summing over the manifold of seven Stark states with $22 \leq n' \leq 28$. In this figure $|\psi_i(x,\tau)|^2$, $i = 1, 2$ and 3 is plotted as a function of x/n^2 in atomic units at scaled times τ. (**a**) $\tau = 0$, (**b**) $\tau = 10$, (**c**) $\tau = 16.3$, (**d**) $\tau = 100$ and (**e**) $\tau = 300$. Here solid line stands for $|\psi_1(x,\tau)|^2$, dotted line stands for $|\psi_2(x,\tau)|^2$ and dashed line stands for $|\psi_3(x,\tau)|^2$.

time τ. Like the originial curves in ref. [9], our curves for both $\langle x\rangle$ and $\langle x^2\rangle$ exhibit fast oscillations with nearly the Kepler period ($t_{\rm cl} = 2.378$ ps) for $n = 25$; the initial states, consistently with the result in figure 2c, show decay and revival with the period $(t_{\rm rev}/2) = (n/3)t_{\rm cl}$. The well-pronounced fast oscillation with a periodicity of half the Kepler period appears to be a common feature of the curves for both $\langle x\rangle$ and $\langle x^2\rangle$.

In figure 4 we present results for $\langle p\rangle$ and $\langle p^2\rangle$ as a function of τ. The plot of $\langle p^2\rangle$ (figure 4b) clearly shows the oscillatory and revival structures as observed in the curves for $\langle x\rangle$ and $\langle x^2\rangle$ in figure 3. The same structures, although not very pronounced, are also present in the curve for $\langle p\rangle$ (figure 4a). In addition to $\langle x\rangle$,

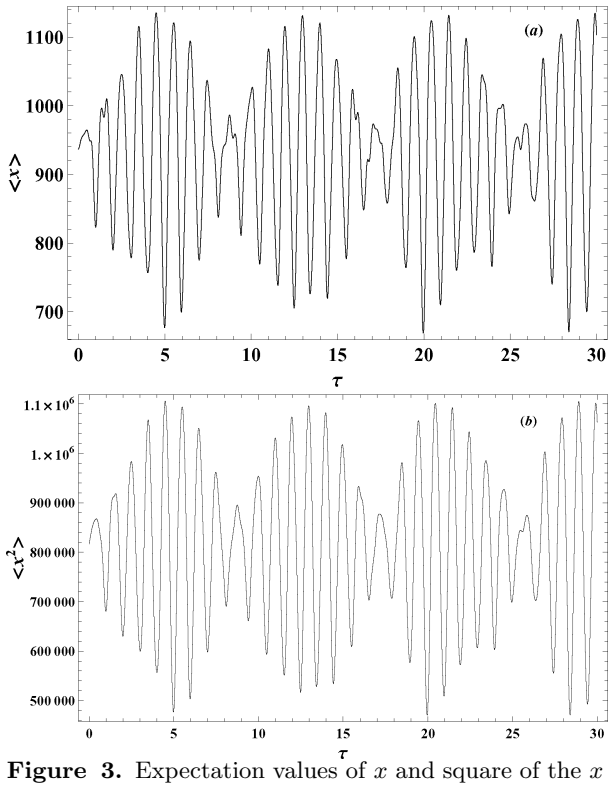

Figure 3. Expectation values of x and square of the x coordinate as a function of scaled time τ. The wave packet was created by an HCP with $q = 0.0016$ a.u. redistributing the initial population to the manifold of seven Stark states with $22 \leq n' \leq 28$. (**a**) Plot of $\langle x \rangle$ and (**b**) plot of $\langle x^2 \rangle$.

$\langle x^2 \rangle$, $\langle p \rangle$ and $\langle p^2 \rangle$, two important physical observables are provided by the widths of the position σ_x and momentum σ_p distributions.

Figure 5 shows the plots of σ_x and σ_p vs. τ. Looking closely into this figure we see that the oscillatory and revival structures are relatively more pronounced in the curve for σ_p (figure 5b) when compared with those in the curve for σ_x (figure 5a). But, a common feature of the curves for σ_x and σ_p is that both minimize simultaneously pointing to the transient phase-space localization of the wave packet. We display in figure 6 the evolution of the uncertainty product. The smallest value of $\Delta x\, \Delta p$ is close to $\frac{1}{2}$ at the initialization time $\tau = 0$. The classical orbital periodicity manifests during the first few orbits until the wave function begins to decohere. The uncertainty product then becomes quite large to take up values as large as 18 before the occurrence of revival. The localization and spreading recur periodically with about the same periodicity as observed in the case of transient phase-space localization.

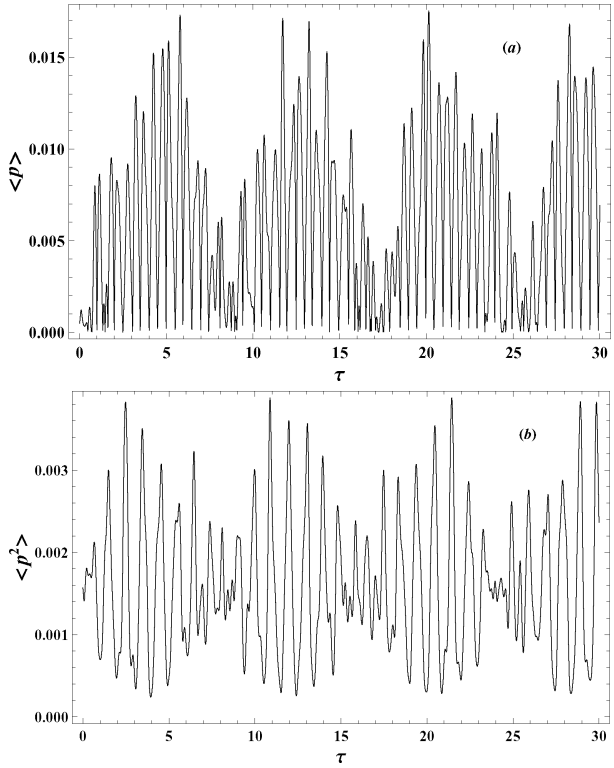

Figure 4. Expectation values of the momentum operators p and p^2 as a function of scaled time τ. The value of q and redistribution of the initial population are the same as those in figure 3. (**a**) Plot of $\langle p \rangle$ and (**b**) plot of $\langle p^2 \rangle$.

4. Conclusion

Because of strong similarities between one- and three-dimensional kicked atoms, it is widely believed that classical-quantum correspondence should be first analysed in one-dimension where accurate quantum calculations may be performed with great confidence. We have followed this viewpoint to study the dynamics of Rydberg wave packets in one-dimensional atoms subject to a unidirectional electric impulse. We have begun by constructing an expression for the matrix element of $n \rightarrow n'$ transition induced by a short HCP in the frame of a quantum mechanical theory and found that there are distinct advantages in using our results to study time dependence of various observables following the application of a kick. For example, the expressions for the expectation values of x, x^2, p and p^2 do not involve, for $n' = n$ and $q = 0$, any unwanted singularity. Note that this singularity does not appear if one works with a semiclassical expression for $T_{n'n}$ [6]. Our construction procedure is based on the use of an exact expression for the terminating confluent hypergeometric function. Recently [14], it was shown that an accurate quantum mechanical result for the matrix element of the radiative dipole transition between

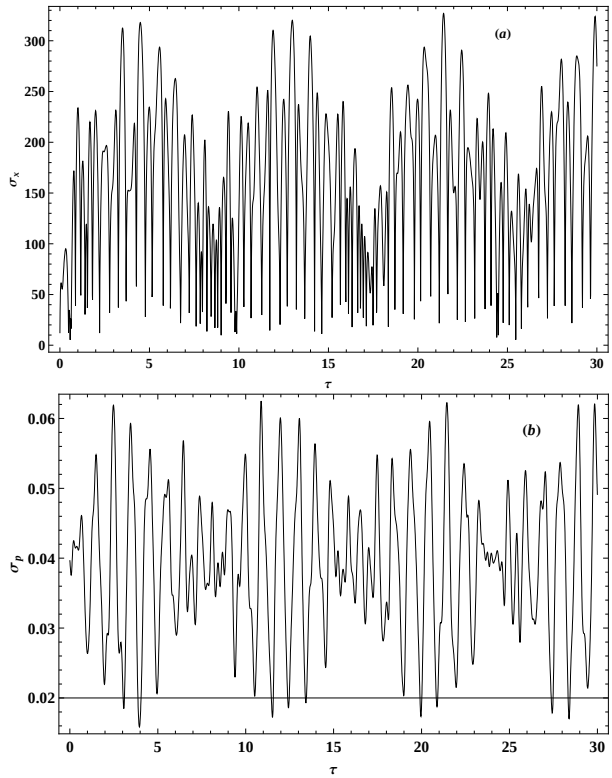

Figure 5. Time development of various observables following the application of a kick of momentum q in atomic units. (**a**) Width of the position distribution σ_x as a function of τ and (**b**) width of the momentum distribution σ_p as a function of τ.

nearby Rydberg states can be obtained by employing an accurate approximation for terminating Gaussian hypergeometric function.

Three time scales, $t_{\rm cl}$, $t_{\rm rev}$, and $t_{\rm sr}$, are supposed to control the evolution and revival of the wave packet. We have studied the revival structure of the Rydberg wave packet with special attention to the time evolution of its components associated with these time scales. Our expressions for $\langle x\rangle$, $\langle x^2\rangle$, $\langle p\rangle$ and $\langle p^2\rangle$ are exact and mathematically uncomplicated such that there is very little numerical inaccuracy in our prediction for phase-space localization of the wave packet. The oscillation of the uncertainty product as a function of the scaled time clearly indicates how the motion of the wave packet in its classical trajectory undergoes a free evolution from classical to quantum and, quantum to classical.

The revival structure arising from different time scales is not a typical property of the Rydberg wave packets only but can be found in many other physical contexts which include coherent states of certain potentials [15] and of various symmetry groups [16]. Revival properties are also displayed by wave packet propagation in nonlinear optical media and in Bose–Einstein condensates [17]. Uncertainty

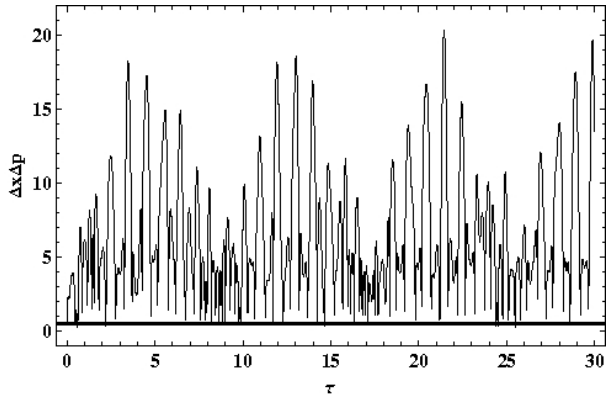

Figure 6. The evolution of the uncertainty product of the Rydberg wave packet. The horizontal dotted line corresponds to $\Delta x \Delta p = \frac{1}{2}$.

principle in quantum mechanics is usually taken to imply that phase-space structure should not exist in a dimension smaller than the Planck constant $\hbar$. In a remarkable paper, Zurek [18] used Wigner distribution function [19] to demonstrate that quantum-chaotic systems develop structures within the sub-Planck scale ($\ll \hbar$). These structures are extremely sensitive to many-body environments that are crucial for the phenomenon of quantum decoherence [20]. Sub-Planck scale structures have been found in many physical systems [21]. There exist detailed studies for the case of superpositions of harmonic-oscillator coherent states. Recently, similar investigations have been extended to generalized coherent states that occur in the time evolution of systems with nonlinear potential at fractional times [22]. More specifically, the signature of sub-Planck scale structure has been found.

Appendix A

As in the case of $x_{n'n}$, the matrix element $p_{n'n} = i\langle n'|\frac{\mathrm{d}}{\mathrm{d}x}|n\rangle$ is calculated by using $|n\rangle$ from (3) but expressing $|n'\rangle$ in terms of the polynomial in (9). The form of $|n\rangle$ clearly indicates that $\frac{\mathrm{d}}{\mathrm{d}x}|n\rangle$ involves the sum of three terms such that the result for $p_{n'n}$ becomes little lengthy. However $p_{n'n}$ can be written in a compact form

$$p_{n'n} = i\alpha_{n'n} \sum_{r'=0}^{n'-1} \beta_{r'n'} \sum_{k=0}^{1} (-1)^{(k+1)} \times \left\{ \frac{\Gamma(m'+k-1)}{y(0)^{m'+k-1}} {}_2F_1\left(1-n+k, m'+k-1, 2+k, \frac{2}{ny(0)}\right) - \frac{1}{n}\frac{\Gamma(m')}{y(0)^{m'}} {}_2F_1\left(1-n+k, m', 2+k, \frac{2}{ny(0)}\right) \right\}. \quad \text{(A1)}$$

Similarly, one can obtain

$$(p^2)_{n'n} = \alpha_{n'n} \sum_{r'=0}^{n'-1} \beta_{r'n'} \times \left\{ \frac{\Gamma(m'-1)}{y(0)^{m'-1}} \left\{ a\, {}_2F_1\left(1-n, m'-1, 2, \frac{2}{ny(0)}\right) + b\, {}_2F_1\left(2-n, m'-1, 3, \frac{2}{ny(0)}\right) \right\} + \frac{\Gamma(m')}{y(0)^{m'}} \times \left\{ c\, {}_2F_1\left(2-n, m', 3, \frac{2}{ny(0)}\right) + d\, {}_2F_1\left(3-n, m', 4, \frac{2}{ny(0)}\right) + e\, {}_2F_1\left(1-n, m', 2, \frac{2}{ny(0)}\right) \right\} \right\}. \quad \text{(A2)}$$

Here $a = -\frac{2}{n}$, $b = 2(\frac{1}{n} - 1)$, $c = 2(\frac{1}{n} - \frac{1}{n^2})$, $d = 2(\frac{2}{3n^2} - \frac{1}{n} + \frac{1}{3})$ and $e = \frac{1}{n^2}$. Expressions (11), (14), (A1) and (A2) via equations like that in (4) are very convenient for evaluating $\langle x \rangle$, $\langle x^2 \rangle$, $\langle p \rangle$ and $\langle p^2 \rangle$ using Wolfram Mathematica [23].

Acknowledgement

This work forms the part of a Research Project (F. No. 32-39/2006(SR)) funded by the University Grants Commission, Government of India. The authors would like to thank Sk. Golam Ali for his kind help in the numerical part of the work.

References

[1] R R Jones, D You and P H Bucksbaum, *Phys. Rev. Lett.* **70**, 1236 (1993)
[2] T C Weinacht, J Ahn and P N Buckabaum, *Nature (London)* **397**, 233 (1999)
J Ahn, T C Weinacht and P H Bucksbaum, *Science* **287**, 463 (2000)
[3] S Yoshida, C O Reinhold and J Burgdörfer, *Phys. Rev. Lett.* **84**, 2602 (2000)
[4] F B Dunning, J J Mestayer, C O Reinhold, S Yoshida and J Burgdörfer, *J. Phys. B: At. Mol. Opt. Phys.* **42**, 022001 (2009)
[5] M T Frey, F B Dunning, C O Reinhold, S Yoshida and J Burgdörfer, *Phys. Rev.* **A59**, 1434 (1999)
[6] I Bersons and R Veilande, *Phys. Rev.* **A69**, 043408 (2004)
[7] J Bromage and C R Stroud, *Phys. Rev. Lett.* **83**, 4963 (1999)
[8] L D Landau and E M Lifshitz, *Quantum mechanics* (Pergamon, Oxford, 1977)
[9] A Wetzels, A Gürtler, H G Muller and L D Noordam, *Eur. Phys. J.* **D14** 157 (2001)
[10] D G Arbó, C O Reinhold, J Burgdörfer, A K Pattanayak, C L Stokely, W Zhao, J C Lancaster and F B Dunning, *Phys. Rev.* **A67**, 063401 (2003)
[11] M Abramowitz and I A Stegan, *Handbook of mathematical functions* (Dover Pub. Inc., New York, 1972)
[12] I S Gradshteyn and I M Ryzhik, *Table of integrals, series and products* (Academic Press, New York, 1980)
[13] R Bluhm, V A Kostelecky and J A Porter, *Am. J. Phys.* **64**, 944 (1996)
[14] D P Dewangan, *J. Phys. B: At. Mol. Opt. Phys.* **36**, 2479 (2003)
[15] U Roy, J Banerji and P K Panigrahi, *J. Phys. A: Math. Gen.* **38**, 9115 (2005)

[16] J Banerji, *Pramana – J. Phys.* **56**, 267 (2001)
[17] C Sudheesh, S Lakshmibala and V Balakrishnan, *Phys. Lett.* **A329**, 14 (2004)
[18] W H Zurek, *Nature (London)* **412**, 712 (2001)
[19] M Hillery, R F O'Connell, M O Scully and E P Wigner, *Phys. Rep.* **106**, 121 (1984)
[20] G S Agarwal and P K Pathak, *Phys. Rev.* **A70**, 053813 (2004)
P K Pathak and G S Agarwal, *Phys. Rev.* **A71**, 043823 (2005)
S Ghosh, U Roy, C Genes and D Vitali, *Phys. Rev.* **A79**, 052104 (2009)
[21] S Ghosh, A Chiruvelli, J Banerji and P K Panigrahi, *Phys. Rev.* **A73**, 013411 (2006)
J R Bhatt, P K Panigrahi and M Vyas, *Phys. Rev.* **A78**, 034101 (2008)
[22] U Ray, S Ghosh, P K Panigrahi and D Vitali, *Phys. Rev.* **A80**, 052115 (2009)
[23] S Wolfram, *Mathematica, a system for doing mathematics by computer* (Wolfram Research Inc., New York, 2007)